Robust Oscillations and Edge Modes in Nonunitary Floquet Systems

Vikram Ravindranath and Xiao Chen
Department of Physics, Boston College, Chestnut Hill, Massachusetts 02467, USA

(Received 9 October 2022; accepted 11 May 2023; published 9 June 2023)

We explore oscillatory behavior in a family of periodically driven spin chains which are subject to a weak measurement followed by postselection. We discover a transition to an oscillatory phase as the strength of the measurement is increased. By mapping these spin chains to free fermion models, we find that this transition is reflected in the opening of a gap in the imaginary direction. Interestingly, we find a robust, purely real, edge π mode in the oscillatory phase. We establish a correspondence between the complex bulk spectrum and these edge modes. These oscillations are numerically found to be stable against interactions and disorder.

DOI: 10.1103/PhysRevLett.130.230402

Introduction.—Recent years have witnessed a growing interest in the monitored many-body quantum dynamics. It has been shown that there exists a generic entanglement phase transition in a unitary quantum dynamics subject to continuous monitoring [1–5]. By varying the monitoring strength, the individual quantum trajectory changes from a highly entangled volume-law phase to a disentangled area-law phase. Besides this phase transition, monitoring quantum dynamics can generate novel quantum phases, which exhibit quantum criticality or even host quantum orders [6–12]. Here the order can be conventional order or topological order, and is determined by the form of the measurement operator.

Most of these studies are focused on the static order in the steady state. In this Letter, we explore quantum ordered phases with oscillatory behavior in a monitored qubit system. We investigate this behavior in a periodically driven nonunitary circuit. We show that the steady state can exhibit persistent oscillations between two ordered phases. Moreover, these oscillations break the discrete time-translation symmetry of the underlying dynamics, similar to time crystals which have been observed in disordered Floquet many-body localized systems [13–16]. In our model, the quantum order is protected by local "forced" measurements that prefer specific ordered configurations. Applied local unitaries flip between these ordered configurations, leading to oscillations.

In systems which can be mapped to models of free fermions, we demonstrate that such an oscillation behavior is due to a non-Hermitian analog of Majorana zero modes. Such an idea has been used to understand the ground state degeneracy in the Ising spin chain [17]. It has further been employed to understand "(almost) strong modes" that exhibit long coherence times in various static and driven Hermitian systems [18,19]. In our model, the zero mode exists in an *imaginary* gap in the spectrum, is localized on the boundary, and anticommutes with the evolution operator, resulting in persistent oscillation behavior.

Nonunitary Floquet dynamics.—The dynamics of periodically driven systems over one period T is governed by the Floquet operator $\hat{V}$ [20]. Analogous to unitary dynamics, in the nonunitary case, the dynamics of the quantum state is given by the repeated application of $\hat{V}$ followed by an explicit normalization of the state,

$$|\psi(NT)\rangle = \frac{\hat{V}(NT)|\psi_0\rangle}{\|\hat{V}(NT)|\psi_0\rangle\|} = \frac{(\hat{V})^N|\psi_0\rangle}{\|(\hat{V})^N|\psi_0\rangle\|}, \tag{1}$$

where T has been set to 1. To understand the properties of the steady states—in the limit $N \to \infty$—we need to analyze the spectrum of the $\hat{V}$ operator.

It is also convenient to define an effective non-Hermitian Hamiltonian $\hat{H}_F$ by expressing $\hat{V}$ as $e^{-i\hat{H}_F}$. We denote the (complex) eigenvalues of $\hat{H}_F$ by $\{E_n\}$, their corresponding right eigenstates by $\{|E_n\rangle\}$, and order them such that $\mathrm{Im}\{E_j\} \geq \mathrm{Im}\{E_{j+1}\}$. A generic initial state can be expressed as

$$|\psi_0\rangle = \sum c_j |E_j\rangle. \tag{2}$$

Under time evolution, the unnormalized state,

$$|\psi(NT)\rangle = \sum_j c_j e^{-iE_j^R N} e^{E_j^I N} |E_j\rangle, \tag{3}$$

where $E_j^{R(I)}$ denotes the real (imaginary) part of E_j. Clearly, as $N \to \infty$, the quantum state approaches $|E_1\rangle$ with the largest E_1^I, provided that $c_1 \neq 0$.

In principle, a degeneracy in the imaginary direction can emerge so that $E_1^I = E_2^I = \cdots = E_{N_S}^I$ for some $N_S \geq 2$. Generic initial states then do not evolve to a single final state; instead, they continue to evolve, even at late times, in the subspace spanned by $\{|E_1\rangle, |E_2\rangle, \ldots, |E_{N_S}\rangle\}$. If the real parts

E_j^R are uniformly separated so that $E_j^R \equiv E_0 + j(2\pi/N_S)$, the steady states can exhibit periodic behavior, with period N_S. In this Letter, we focus on $N_S = 2$.

Free fermions and "zero" modes.—When the Hamiltonian $\hat{H}$ can be mapped to a system of noninteracting fermions, the many-particle spectrum of $\hat{H}$ can be built up by independently filling in the different single-particle energy levels. Since the many-particle energies are the sums of the energies of the occupied levels, a two-dimensional steady-state subspace manifests in the presence of a single-particle mode $c_0^\dagger$, the imaginary part of whose eigenvalue ϵ_0 is 0. We term such modes that exist in the imaginary gap of the spectrum $i0$ *modes*, to distinguish them from the familiar zero modes that exist in a real gap. Many-body eigenstates can be grouped into pairs that differ solely in the occupation of $c_0^\dagger$. States in a pair have energies with the same imaginary part, and real parts offset by ϵ_0.

With this picture in mind, given a $\hat{V}$ which describes noninteracting fermions, the many-body spectrum of $\hat{V}$ is now obtained from the product of its single-particle eigenvalues. A single-particle mode $c_0^\dagger$ with the property that $\hat{V}c_0^\dagger = -c_0^\dagger\hat{V}(=e^{-i\pi}c_0^\dagger\hat{V})$ generates a similar pairing of many-body states which differ in the occupation of $c_0^\dagger$, thereby having eigenvalues with the same absolute value, but differing in sign.

Model and setup.—We consider a system of L spins subject to periodic, nonunitary driving, described by a Floquet operator $\hat{V}$. We study operators $\hat{V}$ which can be written as a composition of an imaginary time evolution $\hat{U}_I$ and a unitary operator $\hat{U}_R$. We also define the non-Hermitian Floqet Hamiltonian $\hat{H}_F$. We consider a specific form for $\hat{U}_I$ and $\hat{U}_R$, as follows:

$$\begin{aligned}
\hat{V} &= \hat{U}_I\hat{U}_R, \\
\hat{U}_I &= e^{\beta\sum_j \hat{Z}_j\hat{Z}_{j+1}}, \\
\hat{U}_R &= e^{-iJ_{zz}\sum_j \hat{Z}_j\hat{Z}_{j+1}} e^{-iJ_{xx}\sum_j \hat{X}_j\hat{X}_{j+1}} e^{-ih_y\sum_j Y_j}, \\
\hat{H}_F &\equiv i\log\hat{V}.
\end{aligned} \tag{4}$$

$\hat{X}_j$, $\hat{Y}_j$, and $\hat{Z}_j$ refer to the Pauli operators acting nontrivially only on the spin at site j. The parameters β, J_{zz}, J_{xx}, and h_y are all real. $\hat{U}_I$ can be interpreted as a forced measurement with β being the strength of the measurement. $\hat{U}_R$ is composed of unitaries that describe nearest-neighbor XX and ZZ couplings and a pulse which rotates each spin by $2h_y$ about the Y axis. The operator $\hat{V}$ has a $\mathbb{Z}_2$ symmetry represented by the parity operator $P = \prod_j \hat{Y}_j$, which represents a simultaneous π rotation of every spin about the Y axis. The time evolution proceeds according to Eq. (1).

In the simplest case, where the pulses are near-perfect π rotations about the Y axis, the nearest-neighbor couplings $J_{xx} = J_{zz} = 0$, and the measurement strength $\beta \to \infty$, we expect to see oscillations between the two ordered phases $|\uparrow\uparrow\uparrow\cdots\rangle$ and $|\downarrow\downarrow\downarrow\cdots\rangle$. Our objective is to study the consequences of moving away from this fine-tuned limit and examine if there exists a phase with finite β in which oscillations are present.

Bulk spectrum.—We begin by studying the single-particle spectrum of the operator $\hat{V}$ with a fixed β. The corresponding noninteracting Hamiltonian H_F has the form $\hat{H}_F = \frac{1}{4}\sum_{i,j}\gamma_i\mathcal{H}_{ij}\gamma_j$, with $\mathcal{H}$ a complex, antisymmetric $2L \times 2L$ matrix and γ_i being Majorana fermion operators. This Hamiltonian can be diagonalized analogously to a Hermitian free fermion system [21], albeit now with a complex spectrum and complex Majorana-like operators g_j:

$$\hat{H}_F = \frac{i}{2}\sum_{j=1}^{L}\epsilon_j g_{2j-1}g_{2j}. \tag{5}$$

Since the $\hat{V}$ (hence also $\hat{H}_F$) that we consider does not conserve particle number, we plot the quasienergy spectrum in pairs of $\pm(\epsilon/2)$, where the $+$ $(-)$ corresponds to a single-particle state being occupied (unoccupied), resulting in $2L$ points being presented on each plot. A many-body eigenstate of $\hat{V}$ is determined by choosing one mode in each of the L pairs. The process of obtaining and diagonalizing $\hat{H}_F$ is detailed in Ref. [22].

We first focus on the regime where β is large. Consequently, the spectrum is gapped for a wide range of h_y. As h_y is varied, an eigenvalue gap closes and reopens in the imaginary direction. With open boundary conditions, $i0$ modes are present on either side of the gap closing. When h_y is small, the modes are degenerate. However, when h_y is tuned through the reopening of the imaginary gap, a π splitting between the real parts of the $i0$ modes emerges, as shown in Fig. 1. This is accompanied by the presence of oscillations in the steady state. The transition that we observe concerns the development of this robust splitting of π in the real values—not merely the presence—of the $i0$ modes.

For the case where $J_{xx} = J_{zz} = 0$, the bulk spectrum of H_F, $\epsilon(k)$ can be obtained analytically:

$$\begin{aligned}
\epsilon(k) &= \frac{i}{2}\log\left[z(k) \pm i\sqrt{1-(z(k))^2}\right], \\
z(k) &= \cosh 2\beta\cos(2h_y) + i\sinh(2\beta)\sin(2h_y)\cos(k).
\end{aligned} \tag{6}$$

The gap closing in the imaginary direction corresponds to $|z \pm i\sqrt{1-z^2}| = 1$. This can only happen at $k = (\pi/2)$, requiring the condition

$$|\cosh(2\beta)\cos(2h_y)| > 1 \tag{7}$$

for the gap to remain open. The phases with and without a π splitting between the real parts of the $i0$ modes'

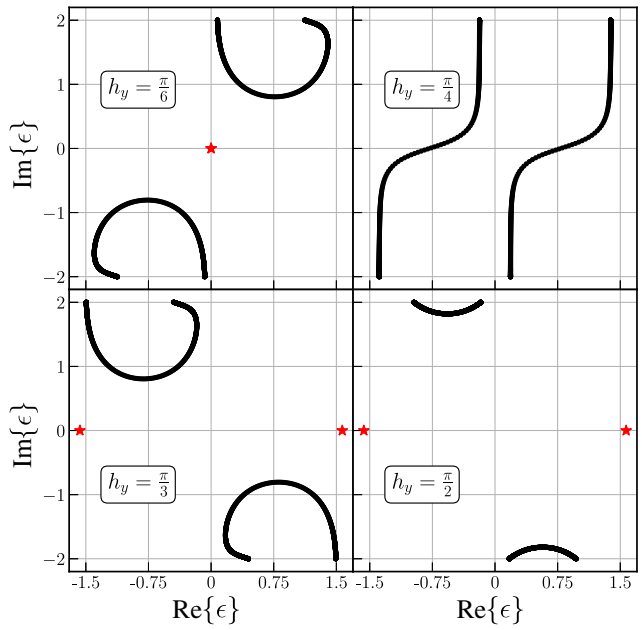

FIG. 1. Complex spectrum of $\hat{H}_F$ given in Eq. (4) with $L = 1000$, $J_{xx} = 0.4$, $J_{zz} = 1$, and $\beta = 2$ with open boundary conditions for various h_y. The imaginary gap closes and reopens with the presence of a π splitting between the $i0$ modes.

energies correspond to $\cosh(2\beta)\cos(2h_y) < -1$ and $\cosh(2\beta)\cos(2h_y) > 1$, respectively.

Edge $i0$ modes.—We now analyze the $i0$ modes and their real-space distribution in detail. We begin by delineating the role of an $i0$ mode. When the imaginary time evolution part of $\hat{V}$ is sufficiently strong, the steady state is superposition of two states $\{|1\rangle, |2\rangle\}$ which have opposite parity and are the right eigenvectors of $\hat{V}$. These are degenerate, in the sense that $\hat{V}|i\rangle = \lambda_i|i\rangle$ for $i = 1, 2$, $|\lambda_1| = |\lambda_2|$ and $|\lambda_1| > |\lambda_j|$ for all other eigenstates $|j\rangle$ $(j \neq 1, 2)$ of $\hat{V}$. An $i0$ mode is an operator $\hat{F}$ that can toggle between $|1\rangle$ and $|2\rangle$.

Since it toggles between states of different parity, $\hat{F}$ anticommutes with $\hat{P}$. Further, since $|\lambda_1| = |\lambda_2|$, $\hat{V}\hat{F} = e^{i\theta}\hat{F}\hat{V}$, with θ real. This can be seen from the effect of $\hat{V}$ on a superposition of $|1\rangle, |2\rangle$, since if θ were complex, there would be only one steady state:

$$\begin{aligned}\hat{V}|\psi\rangle &= \hat{V}(a|1\rangle + b|2\rangle) = \hat{V}(a|1\rangle + b\hat{F}|1\rangle) \\ &= (a\hat{V}|1\rangle + e^{i\theta}b\hat{F}\hat{V}|1\rangle) = \lambda_1(a|1\rangle + e^{i\theta}b|2\rangle). \quad (8)\end{aligned}$$

Further, since this Letter considers models with a two-dimensional steady-state space, we must have $\hat{F}^2|1\rangle = e^{2i\theta}|1\rangle$, and $\hat{F}^2|1\rangle = \hat{F}|2\rangle = |1\rangle$, implying $\theta = 0$ or π. In the case where $\theta = \pi$, oscillations with twice the period of the driving are observed, and $\hat{V}$ and $\hat{F}$ anticommute. There are two $i0$ modes $\hat{F}_{(L)}$ and $\hat{F}_{(R)}$, localized on the left and right boundaries, respectively. The localization of these $i0$ modes guarantees the double degeneracy of the steady states in the thermodynamic limit. For instance, in the limit where $\beta \to \infty$ and $h_y \approx (\pi/2)$, the steady states are $|n\rangle = (1/\sqrt{2})[|\uparrow\uparrow\uparrow\cdots\rangle + (-1)^n i^L|\downarrow\downarrow\downarrow\cdots\rangle]$ for $n = 1, 2$. The role of $\hat{F}_{L(R)}$ is played by $\hat{Z}_{1(L)}$, and both $\hat{Z}_{1,L}$ anticommute with $\hat{V}$.

Summarizing, the $i0$ mode satisfies (1) $\{\hat{F}, \hat{P}\} = 0$, (2) $\{\hat{F}, \hat{V}\} \to 0$ as $L \to \infty$, (3) $\hat{F}$ decays exponentially into the bulk, and (4) $\hat{F} = \sum_{j=1}^{L} v_{2j-1}a_j + v_{2j}b_j$ in free fermion systems.

Additionally, we require that $\hat{F}^2 \propto \mathbb{1}$, since the steady-state space is two dimensional. This condition is trivially satisfied by the ansatz (4) for free fermion systems.

In the parameter regime shown in Fig. 1 with $h_y < (\pi/4)$, there are $i0$ modes as well, except with equal real parts. In this regime, although there are doubly degenerate steady states, oscillations are absent (i.e., $\theta = 0$). These $i0$ modes are obtained by replacing (2) with $[\hat{F}, \hat{V}] = 0$.

For $\hat{F}$, $\vec{v}$ can be computed in the thermodynamic limit by using a transfer matrix method, which proceeds by rewriting the equation $\{\hat{F}, \hat{V}\} = 0$ as

$$\begin{pmatrix} v_{2j+2} \\ v_{2j+1} \end{pmatrix} = T \begin{pmatrix} v_{2j} \\ v_{2j-1} \end{pmatrix}, \quad (9)$$

for $1 \leq j \leq L-2$. Crucially, this equation holds only for the bulk. We can choose to fulfill either the boundary equation which relates v_2 to v_1 (to obtain $\hat{F}_L$) or v_{2L} to v_{2L-1} (in the case of $\hat{F}_R$).

Here, we analytically solve for $\vec{v}$ for $J_{xx} = J_{zz} = 0$. By imposing the boundary conditions for v_1 and v_2, we find that

$$\begin{aligned}\begin{pmatrix} v_{2j} \\ v_{2j-1} \end{pmatrix} &= \lambda_1^{j-1} \begin{pmatrix} \cos(h_y) \\ \sin(h_y) \end{pmatrix}, \\ \lambda_1 &\equiv i\cot(h_y)\coth(\beta). \quad (10)\end{aligned}$$

Requiring that this edge mode decays exponentially fast into the bulk, we have the condition

$$|\lambda_1| < 1 \Rightarrow \cosh(2\beta)\cos(2h_y) < -1, \quad (11)$$

which is *exactly* the condition for the band gap closing in the imaginary direction obtained in Eq. (7). Thus, we have demonstrated a non-Hermitian bulk boundary correspondence. Extensions of Hermitian topological invariants have previously been used in studies that numerically obtained non-Hermitian edge modes [24,25], adding to this correspondence.

We further compare this with the numerical results shown in Fig. 2. For $J_{xx}, J_{zz} \neq 0$, we can also numerically demonstrate that the $i0$ modes are localized on the edges.

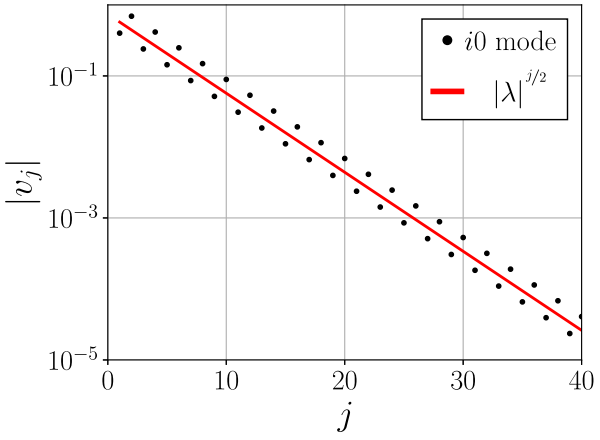

FIG. 2. A plot showing the exponential decay of the $i0$ mode for $L = 1000$, $h_y = (\pi/3)$, and $\beta = 2.0$, compared against the decay rate obtained analytically from Eq. (10).

Lastly, we introduce random spatial inhomogeneity in the Y fields. h_y in Eq. (4) now assumes a position index j, i.e., $h_{y,j} = (\pi/3) \pm \delta\tilde{h}$, where $\tilde{h}$ is uniformly drawn from $[-1, 1]$ for each site. Even in the presence of strong disorder, the $i0$ modes still persist [22], provided that the gap does not close in the imaginary direction.

The robustness of the edge modes requires $L \to \infty$ since the two edge modes can couple in small systems to produce a splitting in both the real and imaginary directions, resulting in a single steady state. The analysis of the splitting with finite L is presented in Ref. [22].

Dynamics and interaction.—We now turn to the dynamics to study the signature of these $i0$ modes. The dynamics can be simulated in two ways: first, by exploiting the mapping to free fermions and using the machinery of fermionic Gaussian states (FGS) [26–31], and second, using matrix product state (MPS) methods [32,33] in terms of the spin degrees of freedom.

A limitation of FGS is that only fermionic states with a definite parity can be simulated. Since $\hat{V}$ conserves parity, the oscillations cannot be observed directly using FGS, since the two steady states $|\psi_\pm\rangle \sim |\uparrow\uparrow\uparrow\cdots\rangle \pm i^L|\downarrow\downarrow\downarrow\cdots\rangle$ have different parities. Instead, beginning with states of different parities, one can show that the final states at long times have an overlap ~ 1 with one of $|\psi_\pm\rangle$, providing indirect evidence for the presence of oscillations. A second limitation is that FGS cannot describe models with interactions. Thus, we use MPS methods to study the dynamics, utilizing the ITensor C++ package [34].

We consider random product initial states $|\psi\rangle_0 = |\uparrow\uparrow\downarrow\uparrow\downarrow\cdots\rangle$, where each spin points up or down along the z axis. This state is stroboscopically evolved using Eq. (1), and the quantity $\langle Z(t)\rangle \equiv (1/L)\sum_j \langle\psi(t)|\hat{Z}_j|\psi(t)\rangle$ is calculated. Oscillations in $\langle Z\rangle$ occur when there are $i0$ modes with a difference of π in the real parts of their quasienergies, and not otherwise (see Fig. 3).

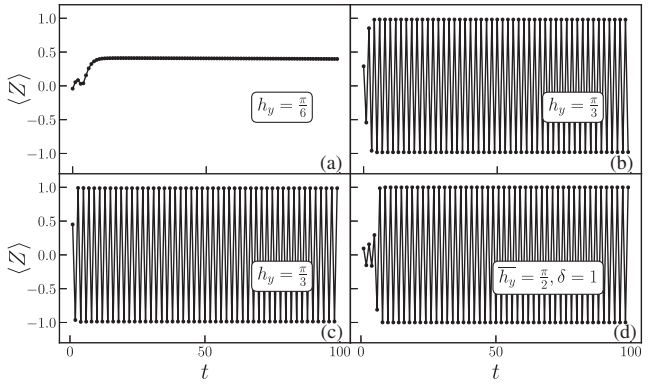

FIG. 3. Plots of $\langle Z\rangle$ without (a),(b) and with interactions [(c),(d), $J_{yy} = 0.3$]. (a) Oscillations are absent and the $i0$ modes are degenerate. (b) Oscillations with double the period are present, and the $i0$ modes show a π splitting. (c) A clean interacting system. (d) A system with strong stochasticity in $h_{y,j}$. In all cases, $J_{xx} = 0.3$, $\beta = 0.75$, $L = 100$.

Interactions are introduced including $e^{-iJ_{yy}\sum_j \hat{Y}_j\hat{Y}_{j+1}}$ in $\hat{U}_R$, which corresponds to a four-fermion interaction $e^{-iJ_{yy}\sum_j \gamma_{2j-1}\gamma_{2j}\gamma_{2j+1}\gamma_{2j+2}}$. Such interactions can lead to thermalization in unitary models, which usually destabilizes any order [35,36]. However, as shown in Fig. 3, oscillations persist in the presence of interactions.

Finally, we consider Y fields that are random in both time and space, modeled as $e^{-i\sum_j h_{y,j}(t)\hat{Y}_j}$, where $h_{y,j}(t) = \overline{h_y} + \delta\tilde{h}_{y,j}(t)$, and $\tilde{h}_{y,j(t)}$ is drawn uniformly from $[-1, 1]$ at every time step. Again, oscillations persist, both in the interacting and the noninteracting models, confirming the stability of the $i0$ mode.

Discussion.—In this Letter, we have studied the emergence of oscillatory behavior in a periodically driven

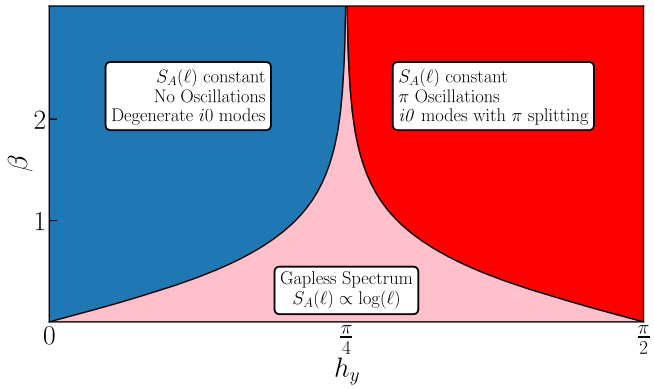

FIG. 4. A phase diagram summarizing the three different phases that are observed as β and h_y are tuned, in the case where $J_{yy} = J_{zz} = J_{xx} = 0$ and the phase boundary is analytically determined. The phase diagram remains qualitatively the same for nonzero J_{xx} and J_{zz}, with possibly more gap closings for larger J_{xx}, J_{zz}. The gapless critical phase is a special feature of nonunitary free fermion dynamics and will be replaced by a volume-law phase in the presence of the interaction, e.g., $J_{yy} \neq 0$.

nonunitary system of qubits. We have found that a critical strength of measurement is required to observe oscillations that break the discrete time-translation symmetry in these systems. Such dynamical behavior is accompanied by the emergence of a non-Hermitian $i0$ mode, which is robust to various perturbations, both quenched and stochastic. Such models can be realized in quantum circuits where one- and two-site unitary gates as in $\hat{U}_R$ are applied to the qubits. The imaginary time evolution can be implemented by subjecting the system to weak measurements corresponding to the following Kraus operators at each site j,

$$M_j^{\pm} = \frac{1}{\sqrt{2\cosh(2\beta)}}[\cosh(\beta) \pm \sinh(\beta)\hat{Z}_j\hat{Z}_{j+1}], \quad (12)$$

and postselecting for the $+$ outcome.

The steady states in either phase studied in the text obey an area-law entanglement scaling. However, there is an intermediate regime between the two steady states where the spectrum is gapless in the imaginary direction. The transition from a regime where there is an imaginary gap in the spectrum of $\hat{H}_F$, to one where there is not, is reflected in a change in the entanglement behavior of the steady states, from an area law to a (parameter-dependent) critical phase [6,7,37]. The properties of this phase are detailed in Ref. [22]. Figure 4 shows the phase diagram for these noninteracting models as both h_y and β are varied.

Whereas we find oscillations even in clean systems, traditional time crystals rely on strong disorder to evade thermalization and thus exhibit order. In our models, the periodic weak measurements may be interpreted as effectively "cooling" the system to the steady-state subspace. The localization of the $i0$ mode on the edge and its spectral gap to bulk states lend additional explanations for this stability [17,38], while unitary time crystals do not rely on such edge modes [13].

In future work, we hope to characterize the $i0$ mode in the presence of interactions. It is possible that such an operator might only pair states in a part of the spectrum of $\hat{H}_F$, but still provide detectable signatures in the dynamics. We would also like to study the role of symmetry breaking in these oscillations, and especially how it might be used to generate oscillations of period greater than 2, and for the case of $N_S > 2$ steady states. Lastly, it would be interesting to understand if analogous $i0$ modes can be found in models that involve a rectification of the system based on measurement outcomes [39].

We gratefully acknowledge computing resources from Research Services at Boston College and the assistance provided by Wei Qiu. This research is supported in part by the National Science Foundation under Grant No. DMR-2219735.

[1] B. Skinner, J. Ruhman, and A. Nahum, Measurement-Induced Phase Transitions in the Dynamics of Entanglement, Phys. Rev. X **9**, 031009 (2019).
[2] Y. Li, X. Chen, and M. P. A. Fisher, Quantum Zeno effect and the many-body entanglement transition, Phys. Rev. B **98**, 205136 (2018).
[3] A. Chan, R. M. Nandkishore, M. Pretko, and G. Smith, Unitary-projective entanglement dynamics, Phys. Rev. B **99**, 224307 (2019).
[4] S. Choi, Y. Bao, X.-L. Qi, and E. Altman, Quantum Error Correction in Scrambling Dynamics and Measurement-Induced Phase Transition, Phys. Rev. Lett. **125**, 030505 (2020).
[5] M. J. Gullans and D. A. Huse, Dynamical Purification Phase Transition Induced by Quantum Measurements, Phys. Rev. X **10**, 041020 (2020).
[6] X. Chen, Y. Li, M. P. A. Fisher, and A. Lucas, Emergent conformal symmetry in nonunitary random dynamics of free fermions, Phys. Rev. Res. **2**, 033017 (2020).
[7] O. Alberton, M. Buchhold, and S. Diehl, Entanglement Transition in a Monitored Free-Fermion Chain: From Extended Criticality to Area Law, Phys. Rev. Lett. **126**, 170602 (2021).
[8] S. Sang and T. H. Hsieh, Measurement-protected quantum phases, Phys. Rev. Res. **3**, 023200 (2021).
[9] A. Lavasani, Y. Alavirad, and M. Barkeshli, Measurement-induced topological entanglement transitions in symmetric random quantum circuits, Nat. Phys. **17**, 342 (2021).
[10] M. Ippoliti, M. J. Gullans, S. Gopalakrishnan, D. A. Huse, and V. Khemani, Entanglement Phase Transitions in Measurement-Only Dynamics, Phys. Rev. X **11**, 011030 (2021).
[11] S. Basu, D. P. Arovas, S. Gopalakrishnan, C. A. Hooley, and V. Oganesyan, Fisher zeros and persistent temporal oscillations in nonunitary quantum circuits, Phys. Rev. Res. **4**, 013018 (2022).
[12] S.-K. Jian, Z.-C. Yang, Z. Bi, and X. Chen, Yang-Lee edge singularity triggered entanglement transition, Phys. Rev. B **104**, L161107 (2021).
[13] V. Khemani, A. Lazarides, R. Moessner, and S. L. Sondhi, Phase Structure of Driven Quantum Systems, Phys. Rev. Lett. **116**, 250401 (2016).
[14] D. V. Else, B. Bauer, and C. Nayak, Floquet Time Crystals, Phys. Rev. Lett. **117**, 090402 (2016).
[15] X. Mi, M. Ippoliti, C. Quintana, A. Greene, Z. Chen, J. Gross, F. Arute, K. Arya, J. Atalaya, R. Babbush *et al.*, Time-crystalline eigenstate order on a quantum processor, Nature (London) **601**, 531 (2022).
[16] J. Randall, C. E. Bradley, F. V. van der Gronden, A. Galicia, M. H. Abobeih, M. Markham, D. J. Twitchen, F. Machado, N. Y. Yao, and T. H. Taminiau, Many-body–localized discrete time crystal with a programmable spin-based quantum simulator, Science **374**, 1474 (2021).
[17] A. Y. Kitaev, Unpaired Majorana fermions in quantum wires, Phys. Usp. **44**, 131 (2001).
[18] J. Kemp, N. Y. Yao, C. R. Laumann, and P. Fendley, Long coherence times for edge spins, J. Stat. Mech. (2017) 063105.

[19] D. J. Yates, F. H. L. Essler, and A. Mitra, Almost strong $(0, \pi)$ edge modes in clean interacting one-dimensional Floquet systems, Phys. Rev. B **99**, 205419 (2019).
[20] L. Reichl, *The Transition to Chaos: Conservative Classical and Quantum Systems* (Springer Nature, Cham, Switzerland, 2021), Vol. 200.
[21] Y.-B. Guo, Y.-C. Yu, R.-Z. Huang, L.-P. Yang, R.-Z. Chi, H.-J. Liao, and T. Xiang, Entanglement entropy of non-Hermitian free fermions, J. Phys. Condens. Matter **33**, 475502 (2021).
[22] See Supplemental Material at http://link.aps.org/supplemental/10.1103/PhysRevLett.130.230402 for details on the diagonalization of non-Hermitian free fermion systems, the transfer matrix method, the implementation of FGS, and the critical phase, which includes Ref. [23].
[23] T.-C. Lu and T. Grover, Spacetime duality between localization transitions and measurement-induced transitions, PRX Quantum **2**, 040319 (2021).
[24] L. Zhou and J. Gong, Non-Hermitian Floquet topological phases with arbitrarily many real-quasienergy edge states, Phys. Rev. B **98**, 205417 (2018).
[25] L. Zhou, Non-Hermitian Floquet topological superconductors with multiple Majorana edge modes, Phys. Rev. B **101**, 014306 (2020).
[26] S. Bravyi, Lagrangian representation for fermionic linear optics, Quantum Inf. Comput. **5**, 216 (2005).
[27] B. M. Terhal and D. P. DiVincenzo, Classical simulation of noninteracting-fermion quantum circuits, Phys. Rev. A **65**, 032325 (2002).
[28] S. Bravyi and R. König, Classical simulation of dissipative fermionic linear optics, Quantum Inf. Comput. **12**, 925 (2012).
[29] J. Surace and L. Tagliacozzo, Fermionic Gaussian states: An introduction to numerical approaches, SciPost Phys. Lect. Notes 54 (2022). 10.21468/SciPostPhysLectNotes.54.
[30] X. Cao, A. Tilloy, and A. D. Luca, Entanglement in a fermion chain under continuous monitoring, SciPost Phys. **7**, 024 (2019).
[31] X. Turkeshi, A. Biella, R. Fazio, M. Dalmonte, and M. Schiró, Measurement-induced entanglement transitions in the quantum Ising chain: From infinite to zero clicks, Phys. Rev. B **103**, 224210 (2021).
[32] S. Paeckel, T. Köhler, A. Swoboda, S. R. Manmana, U. Schollwöck, and C. Hubig, Time-evolution methods for matrix-product states, Ann. Phys. (Amsterdam) **411**, 167998 (2019).
[33] S. R. White and A. E. Feiguin, Real-Time Evolution Using the Density Matrix Renormalization Group, Phys. Rev. Lett. **93**, 076401 (2004).
[34] M. Fishman, S. R. White, and E. M. Stoudenmire, The ITensor Software Library for Tensor Network Calculations, SciPost Phys. Codebases 4 (2022). 10.21468/SciPostPhysCodeb.4.
[35] N. Regnault and R. Nandkishore, Floquet thermalization: Symmetries and random matrix ensembles, Phys. Rev. B **93**, 104203 (2016).
[36] A. Lazarides, A. Das, and R. Moessner, Equilibrium states of generic quantum systems subject to periodic driving, Phys. Rev. E **90**, 012110 (2014).
[37] C.-M. Jian, B. Bauer, A. Keselman, and A. W. Ludwig, Criticality and entanglement in nonunitary quantum circuits and tensor networks of noninteracting fermions, Phys. Rev. B **106**, 134206 (2022).
[38] J. K. Asbóth, L. Oroszlány, and A. Pályi, A short course on topological insulators, Lect. Notes Phys. **919**, 166 (2016).
[39] M. McGinley, S. Roy, and S. A. Parameswaran, Absolutely Stable Spatiotemporal Order in Noisy Quantum Systems, Phys. Rev. Lett. **129**, 090404 (2022).